Science of Sintering, **52** (2020) 339-348

doi:https://doi.org/10.2298/SOS2003339K

UDK: 552.52; 539.217; 622.785

Macroporous Monoliths Based on Natural Mineral Sources, Clay and Diatomite

Maja Kokunešoski[1*)], Miroslav Stanković[2], Marina Vuković[3], Jelena Majstorović[4], Đorđe Šaponjić[1], Svetlana Ilić[1], Aleksandra Šaponjić[1]

[1]Institute of Nuclear Science "Vinča", Institute of National Significance for the Republic of Serbia, University of Belgrade, Belgrade, Serbia

[2]Institute of Chemistry, Technology and Metallurgy, University of Belgrade, Belgrade, Serbia

[3]Institute of Technical Sciences of the Serbian Academy of Sciences and Arts, Belgrade, Serbia

[4]Faculty of Mining and Geology, University of Belgrade, Belgrade, Serbia

Abstract:

Macroporous silica ceramic was obtained using clay and diatomite. Boric acid as a low-cost additive in the amount of 1 wt% was used. These porous materials were obtained at low forming pressure (40-80 MPa) and lower sintering temperature (850-1300 ºC) for 4h in air. The influence of boric acid, forming pressure, and sintering temperature on the microstructure, porosity parameters, and mechanical properties of obtained porous monoliths were investigated. As-received and the modified samples were characterized by X-ray diffraction, FTIR, SEM, and mercury porosimetry measurements. As for modified clay and diatomite, they were pressed at 60 MPa and then sintered at 1150 ºC, obtaining porosities of about 10 % and 60 %, respectively. Both of the analyzed samples had the pore diameter in the range of macroporous materials. The pore diameters of clay samples are ranging from 0.1-10 μm, whereas the pore diameter of diatomite samples was slightly lower with values ranging from 0.05-5 μm. Modified diatomite samples have a lower Young modulus in comparison to modified clay samples.

Keywords*: Sintering; Macroporosity; Clays; Diatomite; Boric acid.*

1. Introduction

In the last few decades, significant progress has been made in the development of porous materials from natural minerals. These new porous materials retain features of the original materials. Porous ceramics provide an opportunity for combining important properties of materials, such as high porosity with high strength and high thermal, mechanical and chemical stability. This combination of properties is very important for various industrial applications in advanced environmental applications as filters, heat insulators, absorbents, catalyst supports, membranes, and chromatography columns [1-14]. Herein, we report the utilization of clay and diatomite or diatomaceous earth as raw materials for the fabrication of macroporous SiO_2 based material. We used economical and green strategy in contrast to complicated processes which are usually applied in the synthesis of porous ceramics [15].

*) **Corresponding author:** majako@vin.bg.ac.rs

Boric acid was used in the amount of 1 wt% which resulted in retaining original porosity (at diatomite) and simultaneously providing consolidation of the materials. The present work is committed to the comparison of various specific properties including measurements of pore size distribution, total intrusion volume, morphology, mechanical properties like Young modulus, and the Poisson ratio of the obtained porous monoliths which became macroporous based on original porosity of clay and diatomite.

It has already been shown in our previously published research papers that higher addition of H_3BO_3 (2 wt%) in the clay and diatomite resulted in a significant increase in their porosity [16-18]. The materials made of modified clay and diatomite opens the possibility of designing materials with desired properties, which will be the subject of our future research.

2. Materials and Experimental Procedures

2.1 Purification procedure and preparation of samples

Clay and diatomite were used as raw materials from the surface coal mine Kolubara, Serbia. Boric acid (Alkaloid AD) was used as an additive.

The same purification procedure has been done for as-received clay and diatomite. As-received materials were purified by using thermal and chemical treatments before processing. Organic impurities have been removed from the materials by heat treatment at 600 °C for 2 h in air. After thermal treatment, as-received materials were chemically treated in an aqueous solution of 0.5 M HCl (p.a. 37 %, BDH Prolabo) (wt% 1:10). Suspensions were stirred for 6 h at 60 ^{o}C. After decanting the liquid phase, residual sediment was dried at 120 °C until the constant weight. The starting mixture was prepared by homogenization of the treated clay and boric acid in the amount of 1 wt%. The saturated aqueous solution of boric acid has been prepared by dissolving boric acid in distilled water at 25 ºC, aided by a magnetic stirrer [19]. The boric acid solution was used in a quantity measured to the solid weight of 1 wt%.

Prepared samples were denoted by C_{a-b} and D_{a-b} following the processing conditions: a-applied pressure and b-sintering temperature while labels for C and D represent clay and diatomite, respectively. The powders were pressed into pellets under different uniaxial pressures: a = 40, 60, and 80 MPa. Pressed samples were sintered: b = 1000, 1150, and 1300 ºC for 4 h in air. The sample sintered at 1000 °C, were damaged and disabled for use in further analyses because of their friable nature.

2.2 Characterization

The chemical composition of as-received clay [16] is shown. Its main composition includes (in wt%) SiO_2–88.00, Al_2O_3–6.05, TiO_2–0.48, Fe_2O_3–2.06, CaO–0.18, MgO–0.35, Na_2O–1.05, and K_2O–1.76. The content of Al_2O_3 is appreciably higher than normal due to the presence of kaolinite in the sample (Chapter 3.1.; PDF no. 89-6538). The chemical composition of as-received diatomite [17] is shown that its main composition includes (in wt%) SiO_2–73.68, Al_2O_3–12.28, Fe_2O_3–3.29, CaO–0.70, MgO–0.44, Na_2O–0.12, and K_2O–1.01. Samples were characterized at room temperature applying X-ray powder diffraction (XRD) technique by using the Ultima IV Rigaku diffractometer, equipped by Cu $K\alpha_{1,2}$ radiation, generator voltage 40.0 kV and current 40.0 mA. The range of 10-60° 2θ was used for all powders in a continuous scan mode with a scanning step size of 0.02° at a scan rate of 5 °/min. The functional groups of samples were studied by using Fourier transform infrared (FTIR) spectroscopy. The powder samples with a small amount of KBr were pressed in a mold and then introduced into a Thermo Scientific iD7 ATR Plates for Nicolet iS5 FT-IR Spectrometer. Spectral data were collected between 1200 and 425 cm^{-1}. The morphology of

clay and diatomite samples was investigated by using the Scanning Electron Microscopy (SEM)-VEGA TS 5130 MM, Tescan. The mercury intrusion porosimetry was applied for measurements of pore size distribution and total intrusion volume. The measurements were performed by automatic porosimeter Fisons-2000 series (limiting pressure 200 MPa and pore diameters from 7.5 to 15000 nm) and Carlo Erba-120 macropore unit (limiting pressure 0.1 MPa and pore diameter from 100.000 to 15.000 nm), and by applying for the data processing program, Milestone 200. Poisson ratio (μ_{din}) and Young modulus (E_{din}) are determined based on measuring ultrasonic velocity. The measurements were performed by using the equipment OYO model 5210, according to the standard testing procedure (SRPS B.B8.12).

3. Results and Discussion

3.1 X-ray diffraction (XRD)

The XRD patterns of as-received and treated clay and diatomite, and $C/D_{60\text{-}1150,\ 1300}$ are shown in Fig. 1. As-received material clay and diatomite were purified by using thermal and chemical treatments.

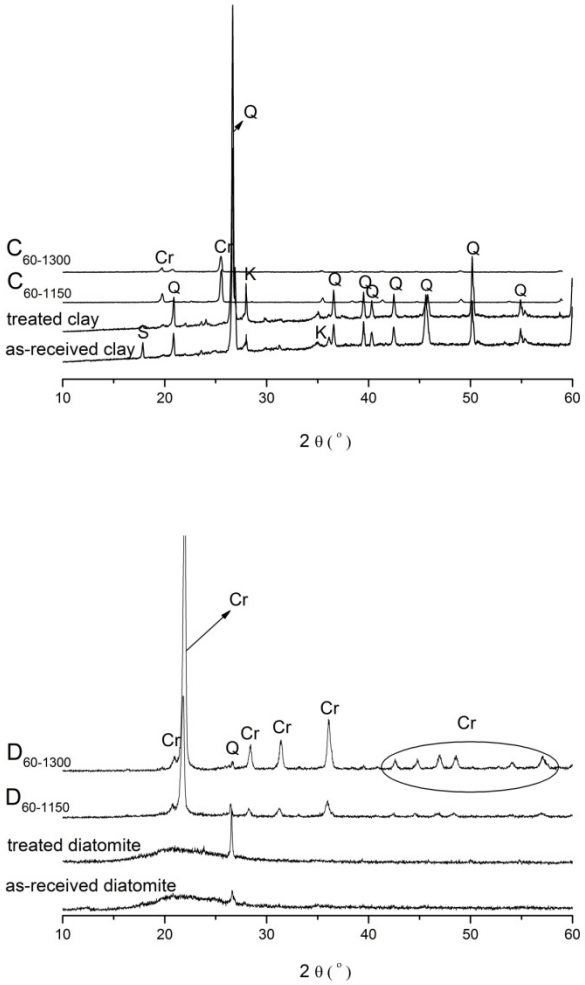

Fig. 1. XRD patterns of as-received and treated clay/diatomite and $C/D_{60\text{-}1150,\ 1300}$;
S smectite (PDF no. 29-1490), **K** kaolinite (PDF no. 89-6538),
Q quartz (PDF no. 33-1161), **Cr** cristobalite (PDF no. 89-3606).

In the X-ray pattern of as-received and treated clay, quartz (PDF no.33-1161) followed by the appearance of clay minerals of kaolinite group, **S** smectite (PDF no. 29-1490), and **K** kaolinite (PDF no. 89-6538) were identified. Cristobalite (PDF no. 82-1410) is formed by recrystallization of quartz and appears in samples $C_{60\text{-}1150}$ and $C_{60\text{-}1300}$ (Fig. 1).

The XRD analysis revealed that the sample of as-received diatomite had a typical opal structure [18, 27, 28]. The XRD pattern shows the broadening of diffraction lines in regions around 15-25º of 2θ, which is associated with the presence of an amorphous silica phase. Cristobalite (PDF no. 82-1410) is the major crystalline phase in the samples sintered at 1150 and 1300 ºC, followed by peaks of quartz (PDF no. 33-1161) [18].

3.2 Fourier transforms infrared (FTIR) spectroscopy

The FT-IR spectra of all investigated clay samples' (Fig. 2) characteristics have a wide band at about 1000 cm^{-1}, which is assigned to Si-O-Si stretching vibrations. A small wide band at 910 cm^{-1} corresponds to Al-OH-Al bending vibrations stemming from OH in the di-octahedral layer, which is observed in the spectrum of as-received clay [20].

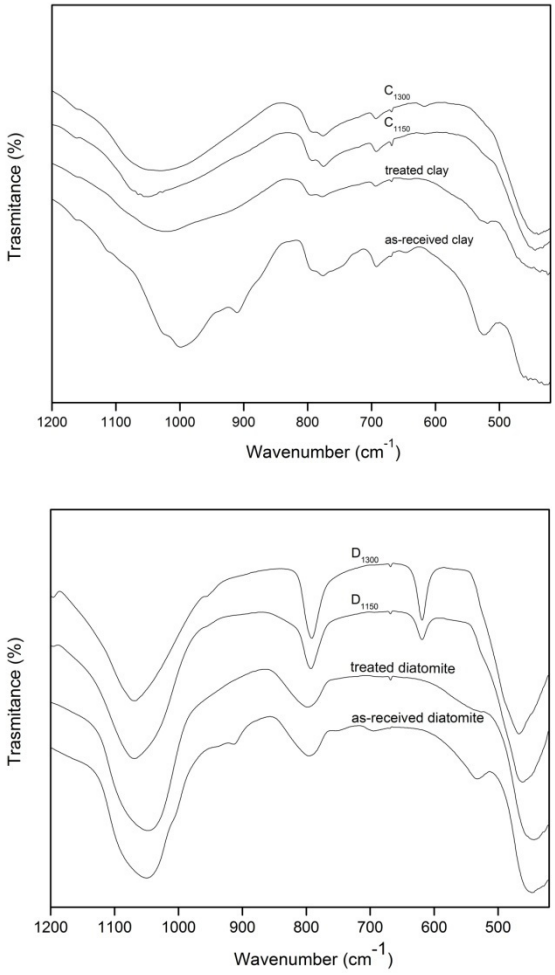

Fig. 2. FT-IR of the as-received, treated clay and diatomite and $C/D_{60\text{-}1150,\ 1300}$.

In the spectrum of all analyzed clay samples, the characteristic band at 795 cm^{-1} is followed by a less intensive band at 775 cm^{-1}, which corresponds to a doublet of quartz [21, 22]. The band at 693 cm^{-1} is assigned to Si-O-Si bending vibrations. The absorption band in

the area around 520 cm^{-1} is observed at the spectrum of as-received and a treated sample is assigned to Si-O-Al bending vibrations stemming from oxygen in the octahedral layer. The wideband at about 440 cm^{-1} originates from the Si-O-Si bending vibrations [22].

In the FT-IR spectrum of all analyzed diatomite samples (Fig. 2) [17] the absorption bands are at about 1050, 800, and 470 cm^{-1} are the characteristic bands for SiO_2 modification associated with the presence of amorphous opal silica phase. A rather weak absorption band is at about 700 cm^{-1} in the spectrum of as-received diatomite indicates that there is a partial arrangement of this SiO_2 modification towards the cristobalite structure which was confirmed by XRD analysis (Section 3.1). The absorption bands at about 1050 and 800 cm^{-1} are assigned to Si-O-Si plane vibrations while the band at about 470 cm^{-1} refers to Si-O-Si deformation vibrations. The weak absorption band at 915 cm^{-1} indicates the presence of clay minerals in as-received diatomite [23-26]. The absorption bands are at ca 620 cm^{-1} in sintered samples, 530 cm^{-1} only in as-received diatomite, and 470 cm^{-1} in the spectrum of all analyzed diatomite samples probably correspond to the combined Si-O (bending) deformation and Al-O stretching vibrations [23-25].

3.3 Scanning electron microscope (SEM)

The microstructures of the polished materials C/D $_{40,60\text{-}1150,\ 1300}$ are shown in Fig. 3. In the SEM images of the clay materials, grains are mostly agglomerated (Fig. 3).

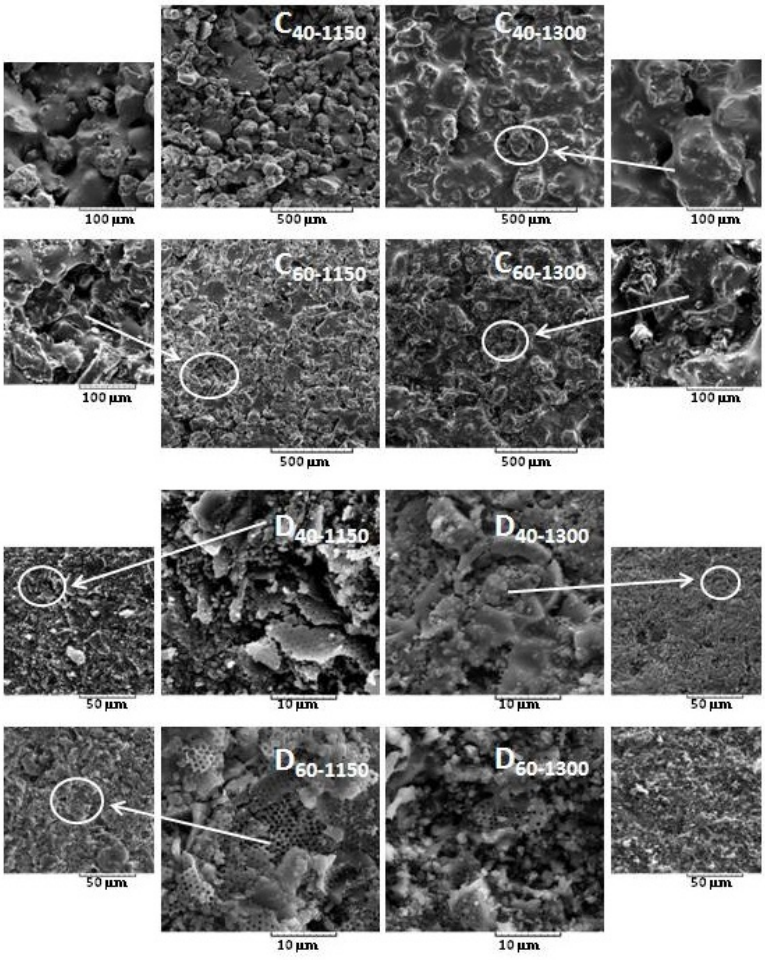

Fig. 3. SEM images of samples C/$D_{40,\ 60\text{-}1150,\ 1300}$.

The surface morphology has a large number of voids and connected pores between irregularly shaped particles. The microstructure of the sample sintered at 1300 ºC showed pore merging for both applied pressures (40 and 60 MPa) [16-18].

The SEM images of diatomite reveal characteristic morphology, the well-known disk, and capsule-shaped frustules with a circular opening in the middle (Fig. 3). Bimodal distribution of pores is easily noticed in the diatomite sample modified with boric acid, resulting from the combination of the inherent fine porosity of the diatomite grains and larger intra-grain pores. The morphology of sintered samples at 1150 and 1300 ºC, still retains some fragments of the original diatomite honeycomb structure [17, 18, 27]. According to SEM images (Fig. 3), which compare the porosity of clay and diatomite samples sintered at 1150 °C which is modified with 1 wt% of boric acid, the clay samples have a significant higher pore diameter than diatomite ones [16-18].

3.4 Mercury intrusion

Fig. 4 shows the pore size distribution curves of the clay/diatomite samples modified with boric acid, pressed at all applied pressure, and sintered at 1150 and 1300 °C, determined by mercury intrusion porosimetry.

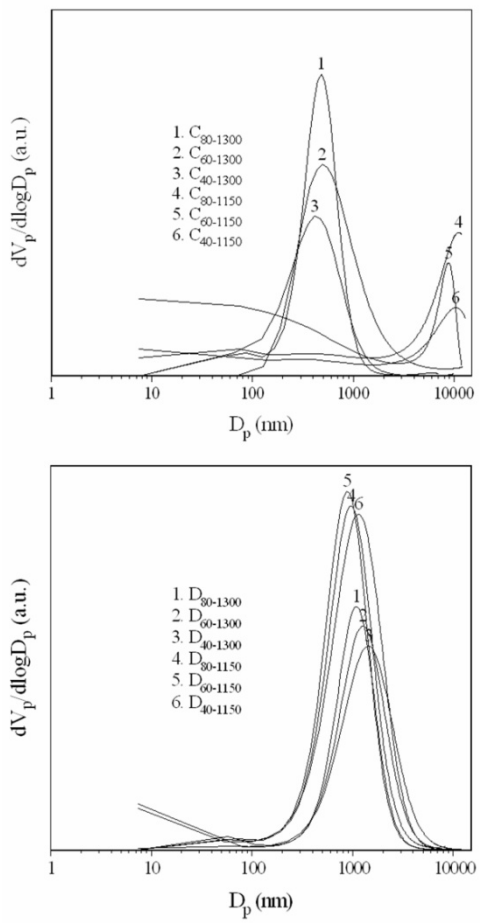

Fig. 4. Pore size distribution versus pore diameter of samples $C/D_{40, 60, 80\text{-}1150, 1300}$.

When it comes to clay samples, the average pore size diameter significantly decreases with the increase of the sintering temperature from 1150 to 1300 °C (Fig. 4). In clay, where

samples are pressed ranging from 40 to 80 MPa and sintered at 1150 °C, the pore size distribution curves are situated from 2.5 μm to over 10 μm which is substantially higher in comparison to the samples obtained at 1300 °C (0.01-2.5 μm). The samples sintered at 1150 °C have weak peaks within the range from 0.03 to 1.5 μm which indicates the presence of a group of smaller diameter pores. The samples sintered at 1300 °C have two shoulders at around 0.1μm (0.05 μm) which also indicates the presence of another group of smaller pores.

The lower values of total pore volume (V_p) and total porosity (P) of the samples sintered at 1150 °C in comparison to the samples obtained at 1300 °C were observed (Tab. I). On the other hand, the average pore diameters (PD) were higher at lower sintering temperature (1150 °C, PD = 9μm – 10 μm) in comparison to the samples sintered at the higher temperature (1300 °C, PD ~ 0.4 μm). Sintering of B_2O_3 and SiO_2 [29] in the presence of impurities in clay [16] leads to melting processes [30-35] which leads to pore merging. Two competitive processes like grain coalescence and pore merging determine the total porosity. At higher temperatures, grain coalescence generally leads to the lowering of V_p, PD and P. Likewise, at higher temperatures pore merging causes large values of V_p and P while PD is lower (Tab. I). It means that the sintered sample at 1300 °C could have a large number of smaller pores compared to the material sintered at 1150 °C resulting in higher values of V_p and P. In the analyzed samples, the boric acid has the role of sintering aid causing the local melting of grain boundaries and particle/grain coalescence, but the net effect of sintering results in increasing of V_p and P at higher temperatures.

The pore size distribution from 0.15 to 10 μm of the diatomite samples with boric acid treated at 1150 and 1300 °C is observed (Fig. 4). The samples sintered at 1150 °C have small peaks ranging from 0.01 to 0.15 μm, which indicates the presence of a group of smaller pores. From the form of curved patterns of the samples pressed at 40 and 80 MPa and sintered at 1300 °C, it can be concluded that these samples have a broad peak below 0.01 μm. Due to better sinterability of diatomite samples caused by finer morphology of as-received diatomite V_p of the samples sintered at 1300 °C were lower compared to the samples sintered at 1150 °C (Fig. 4). Diminution of average pore size in the presence of the applied pressure is observed at the samples obtained at the same temperature (Tab. I). Values of V_p, PD, and P decrease with increasing pressure when it comes to diatomite samples sintered at 1300 °C. For the samples sintered at 1150 °C only P increases with increasing pressure. Due to the finer structure, the specific surface (S_s) of the diatomite samples is significantly higher compared to the clay samples (Tab. I). Measurements confirm the well-known macropore character of the clay and diatomite. These observations are in good agreement with the results obtained by SEM analysis (Section 2.1).

Tab. I Summary of Hg-porosimetry data for samples of $C_{a\text{-}b}/D_{a\text{-}b}$: total pore volume, Vp, specific surface, S_s, average pore diameter, PD, and total porosity, P.

$C_{a\text{-}b}/D_{a\text{-}b}$	V_p, mm^3g^{-1}	S_s, m^2g^{-1}	PD, nm	P, *vol*%
$C_{40\text{-}1150}$	23	0.6	9784	6
$C_{60\text{-}1150}$	43	4.5	8998	11
$C_{80\text{-}1150}$	39	1.2	8998	9
$C_{40\text{-}1300}$	37	0.6	286	9
$C_{60\text{-}1300}$	52	0.9	556	12
$C_{80\text{-}1300}$	51	0.6	438	11
$D_{40\text{-}1150}$	653	6.8	1726	50
$D_{60\text{-}1150}$	609	8.2	1076	57
$D_{80\text{-}1150}$	565	2.9	1554	58
$D_{40\text{-}1300}$	452	5.8	1800	50
$D_{60\text{-}1300}$	416	8.3	1566	46
$D_{80\text{-}1300}$	345	1.6	1394	44

3.5 Young modulus and Poisson ratio

Fig. 5 shows a variation of Young modulus in the presence of forming pressure at 40, 60, and 80 MPa of samples of clay and diatomite with boric acid sintered at 1150 and 1300 ^{o}C.

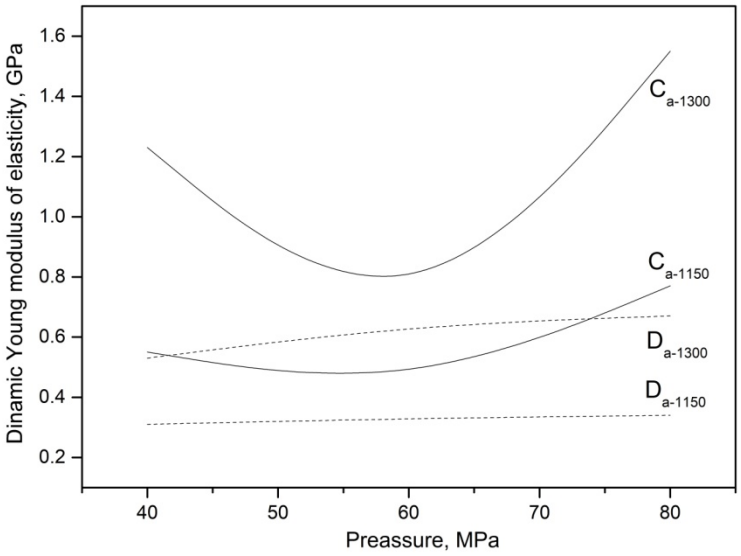

Fig. 5. Young's modulus of samples $C/D_{40,\ 60,\ 80\text{-}1150,1300}$ versus the applied preassure.

The samples $C_{60\text{-}1150,1300}$ have a lower Young modulus in comparison to the samples of $D_{60\text{-}1150,1300}$ (Fig. 5). Young modulus is dependent on the elastic properties of the material and represents the mechanical properties of the material in the macroscopic sense. It is known that Young modulus depends on the phase constitution, shape and size of grains, and the shape and distribution of pores in the material. Young modulus for both groups of samples is variable in a function of the forming pressure. Therefore, the modified clay samples have a generally higher Young modulus in comparison to modified diatomite samples which are caused by lower values of *P* and *Ss* for clay samples (Tab. I). Sintering of B_2O_3 and SiO_2 [29] in the presence of impurities in the clay (Section 2.1) leads to low-temperature eutectic reactions and melting processes [30-34]. The consequences of the local melting are the appearance of the liquid phase at grain boundaries, which produces a glassy phase upon cooling and therefore deteriorates the mechanical properties, like Young modulus [35]. Poisson ratio is ranging from 0.35 to 0.37 for all investigated clay/diatomite samples sintered at 1150 and 1300 ^{o}C [16-18].

4. Conclusion

Macroporous SiO_2 ceramics based on the clay/diatomite were obtained by using an inexpensive method. Boric acid in the amount of 1 wt% was chosen to provide pores during sintering. The samples were pressed at 40, 60, and 80 MPa and sintered from 1000 ºC to 1300 ºC. Porosities of about 10 and 60 % are obtained for the samples of clay and diatomite, sintered at 1150 ºC. As for the clay samples sintered at 1150 ^{o}C, the pore size distribution curves over the entire range of diameters are situated from 2.5 μm to over 10 μm which is higher in comparison to the diatomite samples (0.15-5 μm). In the SEM images of the clay materials, grains are mostly agglomerated with a large number of irregular connected pores

and voids between particles. The SEM images of the diatomite show frustules which have the disk, capsule-shaped with a middle circular opening that is broken due to applied pressure. The porosity of modified diatomite samples remains quite high even though boric acid was added as a sintering aid. Modified diatomite samples generally have a lower Young modulus in comparison to clay samples due to very high values of total porosity and specific surface area which originated from the fine structure of diatomite.

Synthesis of macroporous materials based on the original porosity of clay and diatomite opens the possibility of obtaining composite materials with desired properties. This technique of creating new materials with boric acid can be further developed regarding the potential application of modified clay and diatomite as catalyst or catalyst support in catalytic processes and adsorbents in separation processes.

Acknowledgments

The authors would like to thank Ministry of Education, Science and Technological Development of the Republic of Serbia for financial support of this investigation through projects OI-172045, III-45012 and TR-37021.

5. References

1. J. Nair, P. Nair, J. G. V. Ommen, J. R. H. Ross, A. J. Burggraaf, F. Mizukami, J. Am. Ceram. Soc., 81 (1998) 2709.
2. T. Khalil, F. Abou El-Nour, B. El-Gammal, A. R. Boccaccini AR, Powder Technol., 114 (2001) 106.
3. F. Akhtar, Y. Rehman, L. Bergström, Powder Technol., 201 (2010) 253.
4. S. H. Li, J. R. Wijn, P. Layrolle, K. Groot, J. Am. Ceram. Soc., 86 (2003) 65.
5. S. Ueno, L.M. Lin, H. Nakajima, J. Am. Ceram. Soc., 91 (2008) 223.
6. C. Falamaki, M. Naimi, A. Aghaie, J. Eur. Ceram. Soc., 24 (2004) 3195.
7. F. Akhtar, L. Andersson, S. Ogunwumi, N. Hedin, L. Bergström, J. Eur. Ceram. Soc., 34 (2014) 1643.
8. S. Pandey, V. Buljak, I. Balac, Sci. Sint., 49 (2017) 331.
9. A. Terzić, L. Pezo, Lj. Miličić, N. Mijatović, Z. Radojević, D. Radulović, Lj. Andrić Sci. Sint., 51 (2019) 39.
10. I. Ilić, N. Jović-Jovičić, P. Banković, Z. Mojović, D. Lončarević, I. Gržetić, A. Milutinović-Nikolić, Sci. Sint., 51 (2019) 93.
11. P. Greil, Adv. Mater., 14 (2002) 709.
12. D. J. Green, P. Colombo, MRS Bull 28 (2003) 296.
13. G. M. Dhar, B. N. Snirivas, M. S. Rana, M. Kumar, S. K. Maity, Catal. Today, 86 (2003) 45.
14. B. A. A. L. Van Setten, C. G. M. Spitters, J. Bremmer, A. M. M. Mulders, M. Makkee, J. A. Moulijn, Appl. Catal., B Environ., 42 (2003) 337.
15. P. Sepulveda, J. G. P. Binner, J. Eur. Ceram. Soc., 19 (1999) 2059.
16. M. Kokunešoski, A. Šaponjić, V. Maksimović, M. Stanković, M. Pavlović, J. Pantić, J. Majstorović, Ceram. Int., 40 (2014) 14191.
17. A. Šaponjić, M. Stanković, J. Majstorović, B. Matović, S. Ilić, A. Egelja, M. Kokunešoski, Ceram. Int., 41 (2015) 9745.
18. M. Kokunešoski, A. Šaponjić, M.Stanković, J. Majstorović, A. Egelja, S. Ilić, B. Matović, Ceram. Int., 42 (2016) 6383.
19. C. R. Hammond, Physical constants of inorganic compounds, in: D. R. Lide (Ed.), Hend book of Chemistry and Physics, 84th ed., CRC Press, 2003–2004, pp. 39-166.

20. A. Obut, I. Girgin, Yerbilimleri, 25 (2002) 1.
21. G. E. Christidis, P. W. Scott, A. C. Dunham, Appl. Clay Sci., 12 (1997) 329.
22. J. Madejova, P. Komadel, Clay Clay Miner., 49 (2001) 410.
23. Z. M. Vuković, Modification of porous structure of Ca-smectite, copolymer of glycidyl methacrylate and their composite, Phd. Thesis, University of Belgrade, Faculty of physical chemistry, Belgrade, 2010 (in Serbian).
24. W. T. Tsai, C. W. Lai, K. J. Hsien, J. Colloid Interf. Sci., 297 (2006) 749.
25. V. Poharc-Logar, M. Logar, Geol. An. Balk. Poluos., 62 (1998) 233 (in Serbian).
26. A. Šaponjić, Synthesis and characteristics of Si-non oxide compounds obtained by carbothermal reduction of diatomaceous earth, Phd. Thesis, University of Belgrade, Faculty of mining and geology, Belgrade, 2011 (in Serbian).
27. B. Matović, A. Šaponjić, A. Devečerski, M. Miljković, J. Mater. Sci., 42 (2007) 5448.
28. B. Matović, A. Šaponjić, S. Bošković, J. Serb. Chem. Soc., 71 (2006) 677**.**
29. T. J. Roccket, W. R. Foster, J. Am. Ceram. Soc., 48 (1965) 75.
30. E. T. Carlson, The system $CaO\text{-}B_2O_3$, Bur. Stand. J. Res., 9 (1932) 825.
31. G. W. Morey, H. E. Merwin, J. Am. Ceram. Soc., 58 (1936) 2248.
32. A.P. Roller, C.R. Acad. des Sci. Paris., 200 (1935) 1763.
33. R.B. Sosman, H.E. Merwin, Wash. Acad. Sci. J. 6 (1916) 532.
34. H. V. Wartenberg, H. J. Reusch, E. Saran, Z. Anor. und All. Chem. 230 (1937) 257.
35. Daithı´ deFaoite, D. J. Browne, F. R. Chang-Dı´az, K. T. Stanton, J. Mater. Sci., 47 (2012) 4211.

Сажетак: *Синтетисана је макропорозна керамика на бази силике применом глине и дијатомеје као полазних сировина. Као јефтин адитив коришћена је борна киселина у количини од 1 мас.%. Синтетисани порозни материјали добијени су на ниским притисцима формирања (40-80 MPa) и ниским температурама синтеровања (850-1300 ºC), 4 сата на ваздуху. Проучен је утицај борне киселине, ниског притиска формирања и ниске температуре синтеровања на микроструктуру, параметре порозности и механичке особине добијених монолита. Полазни и модификовани узорци карактерисани су инфрацрвеном спектроскопијом са фуријеовом трансформацијом, рендгенском дифракционом анализом, скенирајућом електронском микроскопијом и живином порозиметријом. За модификоване узорке пресоване на 60 MPa и синтероване на 1150 ºC добијена порозност је око 10% за модификовану глину, а за модификовану дијатомеју око 60 %. Пречник пора код добијених узорака глине је у опсегу 0,1-10 μm, док је код добијених узорака дијатомеје пречник пора у опсегу 0,05-5 μm. Модификовани узорци дијатомеје имају ниже вредности Јунговог модула у односу на модификоване узорке глине.*

Кључне речи*: синтеровање; макропорозност; глина; дијатомеја; борна киселина.*